Available online at www.sciencedirect.com
SCIENCE DIRECT
Journal of Molecular Catalysis A: Chemical 255 (2006) 254–259
JOURNAL OF MOLECULAR CATALYSIS A: CHEMICAL
www.elsevier.com/locate/molcata

Dispersion, reduction and catalytic properties of copper oxide supported on $Ce_{0.5}Zr_{0.5}O_2$ solid solution

Hongliang Chen [a], Haiyang Zhu [a], Yong Wu [a,b], Fei Gao [a], Lin Dong [a,*], Junjie Zhu [a,*]

[a] *Key Laboratory of Mesoscopic Chemistry of MOE, School of Chemistry and Chemical Engineering, Nanjing University, Nanjing 210093, PR China*
[b] *Department of Chemistry, Nanjing Normal University, Nanjing 210097, PR China*

Received 14 November 2005; received in revised form 4 April 2006; accepted 5 April 2006
Available online 22 May 2006

Abstract

$Ce_{0.5}Zr_{0.5}O_2$ solid solution was synthesized by a microwave method and used as support for preparing a series of $CuO/Ce_{0.5}Zr_{0.5}O_2$ catalysts. The samples were characterized by X-ray diffraction (XRD), transmission electron microscopy (TEM), Brunauer-Emmett-Teller (BET) and temperature-programmed reduction (TPR), and the results indicated that: (1) the dispersion capacity of copper oxide on $Ce_{0.5}Zr_{0.5}O_2$ is about 0.70 mmolCuO/100 $m^2Ce_{0.5}Zr_{0.5}O_2$; (2) there are two kinds of copper species in the catalysts, i.e., dispersed and crystalline copper species. The catalytic activities of $CuO/Ce_{0.5}Zr_{0.5}O_2$ for the low temperature (100 and 125 °C) CO oxidation were also tested, which showed that the sample with CuO loading amount of 1.2 mmolCuO/100 $m^2Ce_{0.5}Zr_{0.5}O_2$ presented the highest activity. Combined with the XRD and TPR results, it seems to suggest that the main active species in this system should be the surface and/or small particle copper oxide species.

Keywords: Copper oxide; Microwave; Dispersion capacity; Ceria–zirconia; Solid solution

1. Introduction

In recent years, lots of catalysts have been investigated for the CO catalytic oxidation at low temperature due to its wide applications in pollution control devices for vehicle exhaust, CO gas sensors, catalytic combustion and gas purification of CO_2 lasers [1]. Among of them, the cheap transitional metal oxide catalysts show favorable catalytic activities and special attentions have been paid to the substitution of noble metal catalysts by these systems [2–8].

Copper-contained catalysts show a potential activity for the CO oxidation and have been extensively investigated during the past decades [9–11]. For example, the CuO/CeO_2 catalyst was reported to be very active for the CO oxidation and the results indicated that the activity of CuO/CeO_2 was several orders of magnitude higher than that of conventional Cu-based catalysts and even comparable or superior to noble metals catalysts [12].

On the other hand, ceria has been proved to be a very important and potential component in the three-way catalysts (TWCs) for its unique redox properties and high "oxygen storage capacity" (OSC), which is crucial for controlling the ratio of oxidants and reductants in the automotive exhaust (NO_x, CO, CH_x, etc.) [13]. Ceria is suggested to have these uses in: increasing the thermal stability of the metal oxide support; promoting the noble metal dispersion, the water gas shift (WGS) and steam reforming reactions, and CO removal through oxidation employing a lattice oxygen; favoring catalytic activity at the interfacial metal-support sites; storing and releasing oxygen under lean and rich conditions, respectively [14]. However, as a support, ceria will result in significant efficiency decrease of the catalysts under thermally harsh environments, such as loss of surface area of the support, sintering of precious metals and deactivation of ceria [15]. In order to improve the property of ceria, zirconia is widely used as a promoter in ceria-contained catalysts. After calcinations at high temperature (800 °C), compared to pure ceria, ceria–zirconia mixed oxides shows enhanced redox and oxygen storage properties, improved thermal resistance and better catalytic activity at lower temperature [16,17]. Many methods have been used to prepare the ceria–zirconia solid solution, such as,

* Corresponding authors. Tel.: +86 25 83594945; fax: +86 25 83317761.
E-mail addresses: donglin@nju.edu.cn (L. Dong), jjzhu@mail.nju.edu.cn (J. Zhu).

1381-1169/$ – see front matter © 2006 Elsevier B.V. All rights reserved.
doi:10.1016/j.molcata.2006.04.015

surfactant-assisted approach [16], high-energy milling of a mixture of the oxides [18], and sol–gel techniques [19]. Recently, as a heating method, microwave irradiation has been widely used to fabricate novel functional materials, such as radial arrays composed of prismatic antimony trisulfide whiskers, Te nanorods, and MFI zeolite crystals with a fibrous morphology [20–22]. Date and co-workers prepared the $Ce_{0.75}Zr_{0.25}O_2$ using KOH as precipitator via microwave–hydrothermal method; however, this method requires relatively high pressure [23]. Martínez-Arias et al. investigated the redox properties and catalytic activities for CO oxidation in presence of NO of $CuO/Ce_{0.5}Zr_{0.5}O_2$ with low loading amount of copper species (1 wt%), and they proposed that the two basic factors affecting the catalytic performance of this system were the facility for achieving a partially reduced state for the copper oxide phase at the interfacial zone and the redox properties of the $CuO_x/Ce_{0.5}Zr_{0.5}O_2$ interface [24]. Despite of many studies on ceria–zirconia solid solution and the CuO supported on ceria–zirconia solid solution mentioned above, the nature of interaction between the active species (copper oxide) and the support (ceria–zirconia solid solution) is still indistinct and widely open to study.

In this paper, $Ce_{0.5}Zr_{0.5}O_2$ solid solution were synthesized by a microwave assisted solution-phase heating method and then used as support for a series of $CuO/Ce_{0.5}Zr_{0.5}O_2$ catalysts. The attention is focused on (1) the dispersion of copper oxide on $Ce_{0.5}Zr_{0.5}O_2$; (2) the influence of the copper oxide loading amount on the catalytic activity of these catalysts in low temperature CO oxidation.

2. Experimental

2.1. Catalyst preparation

Appropriate amount of $(NH_4)_2Ce(NO_3)_6$, $Zr(NO_3)_4{\cdot}5H_2O$, hexamethylenetetramine and poly(ethylene glycol)-20000 (PEG) were introduced into 100 mL distilled water to give final concentrations of 0.01 mol/L $(NH_4)_2Ce(NO_3)_6$, 0.01 mol/L $Zr(NO_3)_4{\cdot}5H_2O$, 1.8 wt% hexamethylenetetramine and 1 wt% PEG-20000. Then the mixture was placed into the microwave reflux system and refluxed under ambient air for 10 min. The microwave oven followed a working cycle of 12 s on and 10 s off. After cooling to room temperature, the precipitates were centrifuged, washed with distilled water and ethanol, dried in air, and calcined in flowing air at 500 °C for 4 h. The final product was obtained and characterized by X-ray diffraction (XRD), transmission electron microscopy (TEM) and Brunauer-Emmett-Teller (BET). The result of X-ray fluorescence spectrometer showed that the molar ratio of Ce and Zr was 1.02. The BET surface area of $Ce_{0.5}Zr_{0.5}O_2$ was 68.8 m^2/g. The $Ce_{0.5}Zr_{0.5}O_2$ was hereafter denoted as CZ.

The CuO/CZ catalysts were prepared by impregnating of CZ with an aqueous solution containing requisite amount of $Cu(NO_3)_2{\cdot}5H_2O$ followed by drying at 100 °C and then calcining at 500 °C in air for 2 h. For simplicity, $CuO/Ce_{0.5}Zr_{0.5}O_2$ samples were signed as xCuO/CZ, i.e., 03CuO/CZ corresponds to a sample with CuO loading amount of 0.3 mmolCuO/100 m^2CZ.

2.2. Instrument

The microwave synthetic experiments were performed in a modified National frequency-convertible microwave oven (NN-S570MFS). A reflux system was connected to the microwave oven.

X-Ray diffraction qualitative and quantitative analysis were carried out on a Philips X'pert Pro diffractometer using Ni-filtered Cu Kα radiation (0.15418 nm). The X-ray tube was operated at 40 kV and 40 mA.

Brunauer-Emmett-Teller surface areas were measured by nitrogen adsorption at 77 K on a Micrometrics ASAP-2000 adsorption apparatus.

Quantitative temperature-programmed reduction (TPR) was measured by a pulse equipment, and 100 mg sample was used for each test. Prior to the reduction, the catalyst was pretreated in a N_2 stream at 100 °C for 1 h and then cooled to room temperature. After that, 0.311 mL H_2 was pulsed to the quartz U-tube reactor every time, and the pulse followed a working cycle of 10 s on and 60 s off. A thermal conductivity cell was used to detect the residual H_2 and the temperature was increased linearly at a rate of 2.5 °C/min. For quantitative measure of copper species in the catalysts, the area of the consumed H_2 corresponding to 10 mg pure CuO was used as reference.

X-ray photoelectron spectroscopy (XPS) results were obtained by using a V.G. Escalab MK II spectrometer equipped with a hemispherical electron analyzer. The system was operated at 13 kV and 20 mA using a magnesium anode (Mg Kα, $E = 1253.6$ eV). A binding energy (BE) of 284.5 eV for the C 1 s level was used as an internal reference.

The catalytic activities for CO oxidation were determined in steady state involving a feed steam with a fixed composition 1.6% CO, 20.8% O_2 and 77.6% N_2 by volume. A quartz tube was used as the reactor and the requisite quantity of catalyst (25 mg) was used. The reactions were carried out at 100 and 125 °C with a space velocity of 30000 mL g^{-1} h^{-1}. Two chromatogram columns and thermal conduction detection (TCDs) were used to analyze the products. Column A was packed with 13× molecular sieve for separating O_2, N_2 and CO and column B with Porapak Q for monitoring CO_2.

3. Results and discussion

Fig. 1 shows the XRD pattern of CZ calcined at 500 °C. The results suggest that a cubic fluorite-type phase of $Ce_{0.5}Zr_{0.5}O_2$ has formed and the lattice parameter obtained from the calculation of the (1 1 1) peak is 0.525 nm, which is in agreement with the product of CZ obtained from other route [25]. In addition, the average particle size of the solid solution is calculated to be about 9 nm according to the Debye–Scherrer equation.

As shown in Fig. 2, the TEM image reveals that the product presents sphere-shaped morphology with diameters 10–15 nm, which is basically accordance with the result calculated from the XRD pattern.

The XRD patterns of a series of CuO/CZ catalysts with different CuO loading are presented in Fig. 3. For samples with low CuO loading (≤0.6 mmolCuO/100 m^2CZ), i.e., Fig. 3(a and b),

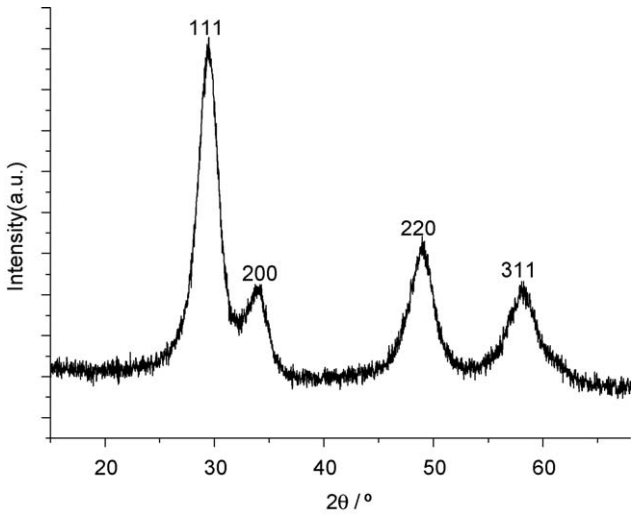

Fig. 1. XRD pattern of CZ calcined at 500 °C.

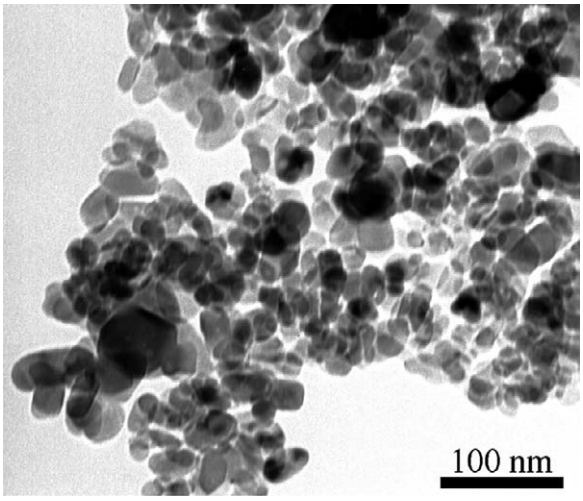

Fig. 2. TEM image of CZ calcined at 500 °C.

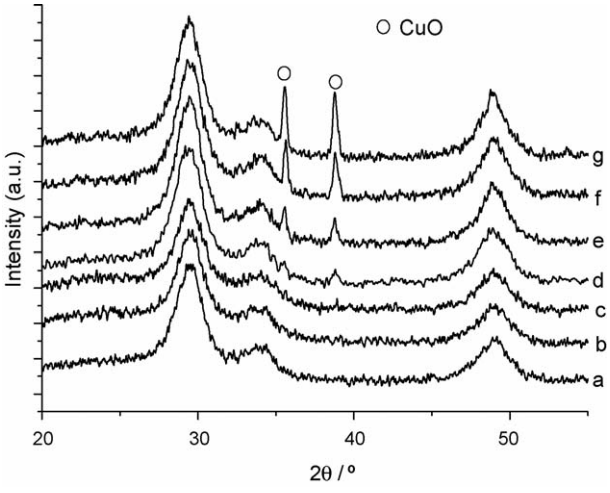

Fig. 3. XRD patterns: (a); (b); (c); (d); (e); (f); and (g), for CuO/CZ with copper oxide loading amounts of 0.3, 0.6, 0.9, 1.2, 1.8, 2.4, and 3.0 mmolCuO/100 m^2CZ, respectively.

no characteristic peaks of crystalline CuO ($2\theta = 35.5$ and 38.7°) has been observed, which suggests that the copper species have been highly dispersed on the surface of CZ. For samples with high CuO loading, the typical diffraction peaks of crystalline CuO have been found, as shown in Fig. 3(c–g), and the intensity of these peaks increases with the CuO loading, indicating the formation of crystalline CuO. XRD quantitative analysis result is shown in Fig. 4 and the dispersion capacity of copper oxide on CZ is around 0.70 mmolCuO/100 m^2CZ.

As discussed elsewhere [26], the solid solution of CeO_2 and ZrO_2 has a fluorite structure and the (1 1 1) plane, which is thermodynamically most stable face and has cubic vacant sites, is preferentially exposed on the surface of CZ. Along this line, the dispersion capacity of CuO on CZ as well as the existing states of the highly dispersed copper species can be estimated by using the incorporation model proposed previously [27]. For CeO_2, the vacant site density on (1 1 1) plane is about 1.22 mmol/100 m^2CeO_2 [28], while for t-ZrO_2, the vacant site density on (1 1 1) plane is about 1.44 mmol/100 m^2ZrO_2 [29]. Considering the lattice parameter ($a = 0.525$ nm) obtained from the XRD result, the vacant site density of (1 1 1) plane of CZ could be calculated about 1.39 mmol/100 m^2CZ. When CZ was impregnated by $Cu(NO_3)_2$ aqueous solution, Cu^{2+} ions would occupy the vacant site on the surface of CZ and the two accompanying NO_3^- anion would stay at the top of the occupied site as capping NO_3^-, compensating the extra positive charge. As reported elsewhere [30], the effect radius and area of NO_3^- is about 0.19 nm and 0.125 nm^2, respectively. The two accompanying NO_3^- anions would prevent some of the neighboring vacant sites on the surface of CZ. During the calcinations, dispersed $Cu(NO_3)_2$ would decompose and form dispersed CuO species and the excess of $Cu(NO_3)_2$ in these samples would decompose and might mainly form crystalline CuO. The schematic diagram for the incorporated Cu^{2+} ions in the surface vacant sites on the (1 1 1) plane of CZ was shown in Fig. 5. Accordingly, for the CuO/CZ samples, the dispersion capacity of copper oxide on CZ is basically equal to the dispersion capacity of $Cu(NO_3)_2$ on

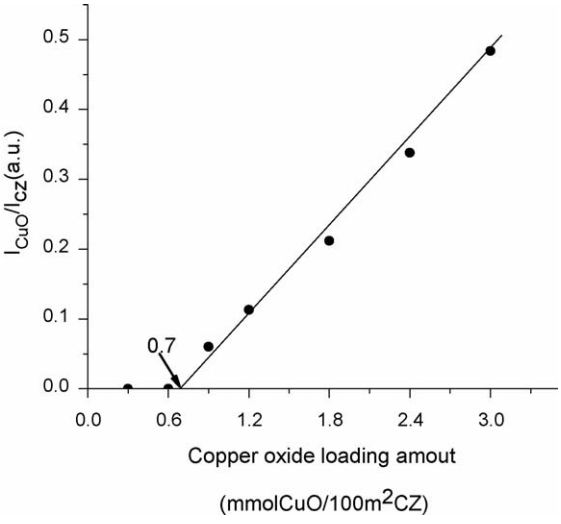

Fig. 4. Quantitative XRD result of CuO/CZ.

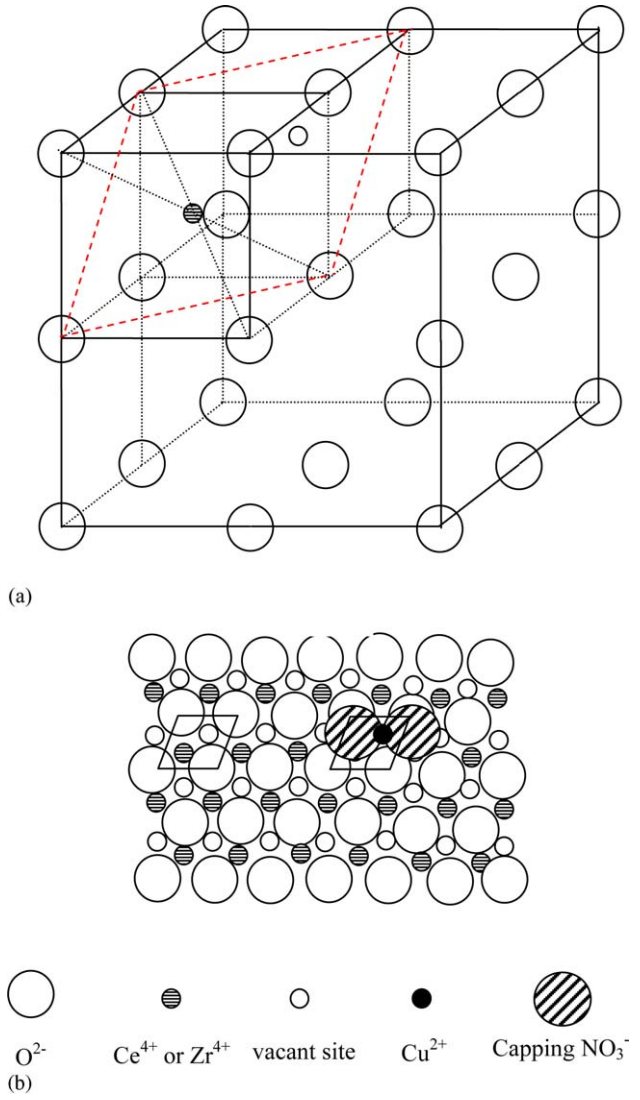

Fig. 5. The schematic diagram for the incorporated Cu^{2+} ions in the surface vacant sites on the (1 1 1) plane of CZ: (a) the schematic diagram of crystal structure of CZ and (b) incorporation of the dispersed Cu^{2+} species accompanying with two NO_3^- anions on the (1 1 1) plane of the CZ support.

CZ, i.e., around 0.66 mmolCuO/100 m^2CZ, which is basically coincided with the XRD result.

TPR profiles of CuO/CZ samples with CuO loading ranging between 0.3 and 3.0 mmolCuO/100 m^2CZ are shown in Fig. 6. For all samples, there are two reduction peaks at approximately 170 and 235 °C and quantitative analysis for these two peaks is carried out, as presented in Table 1. It is interesting that the ratio of the areas of these two peaks is almost constant, which suggests that these two reduction peaks might be attributed to the stepwise reduction of surface dispersed CuO species, i.e., $Cu^{2+} \rightarrow Cu^{+}$ and $Cu^{+} \rightarrow Cu^{0}$ [31]. In addition, H_2 consumption of the peak at 235 °C (from the reduction of Cu^{1+} to Cu^0) is larger than that of the peak at 170 °C (from the reduction of Cu^{2+} to Cu^{1+}), it may be ascribed to the reduction of Cu^{1+} to Cu^0 occurring before the end of the former one due to the influence of H_2 spillover as reported elsewhere [32]. Moreover, the intensities of these peaks increase with CuO loading up to the dispersion capacity. When the CuO loading exceeds the dispersion capacity (Fig. 6(c–g)), the intensities of these two peaks remain basically constant, while a new peak can be observed at approximately 300 °C, the intensity of this peak gradually increases with CuO loading from 0.9 to 3.0 mmolCuO/100 m^2CZ. By comparison with the TPR profile of pure CuO (Fig. 6(h)), the peak at 263–309 °C can be assigned to the reduction of crystalline CuO. In addition, for the CuO/CZ catalyst with the CuO loading amount of 0.9 mmol/100 m^2, small crystalline CuO particle would form in this sample, which could closely contact with the support compared to large crystalline CuO particle. The reduction temperature of small crystalline CuO particle is lower than that of large crystalline CuO particle due to the promotion of support, as shown in Fig. 6(c–g). It can be clearly seen that the reduction temperature of crystalline CuO in CuO/CZ samples shifts to high temperature with CuO loading from 0.9 to 3.0 mmolCuO/100 m^2CZ, which may be explained by that the size of the crystalline CuO increases with copper oxide loading amount. The TPR quantitative results of CuO/CZ, as presented in Table 1, suggest that the dispersion capacity of copper oxide on CZ is about 0.63 mmolCuO/100 m^2CZ, which is basically

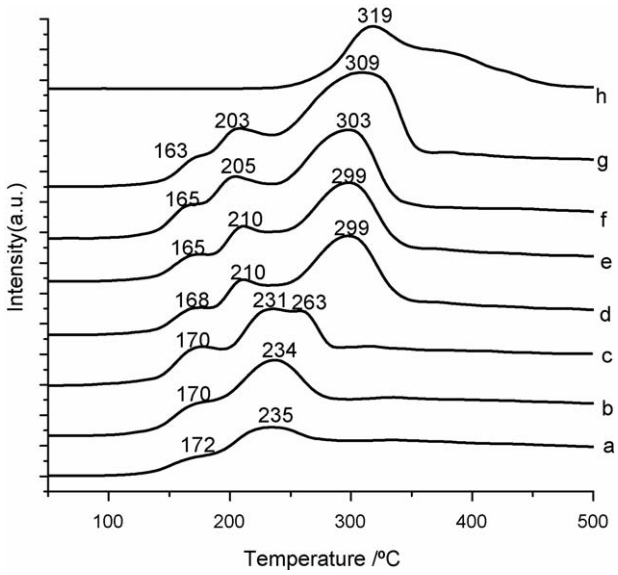

Fig. 6. TPR profiles of CuO/CZ: (a–g) CuO/CZ with copper oxide loading amounts of 0.3, 0.6, 0.9, 1.2, 1.8, 2.4, and 3.0 mmolCuO/100 m^2CZ, respectively; (h) crystalline CuO.

Table 1
Quantitative TPR results of CuO/CZ

CuO loading (mmolCuO/100 m^2CZ)	The ratio of the area of the first peak and the second peak	H_2 consumption	
		Dispersed copper (area percent)	Crystalline copper (area percent)
0.3	1:2.43	100.0%	0
0.6	1:2.45	100.0%	0
0.9	1:2.32	68.1%	31.9%
1.2	1:2.41	42.2%	57.8%
1.8	1:2.38	28.9%	71.1%
2.4	1:2.34	24.7%	75.3%
3.0	1:2.42	20.9%	79.1%

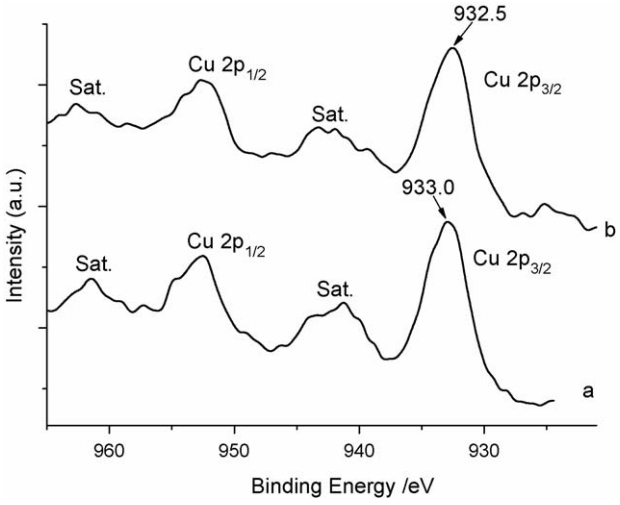

Fig. 7. Cu2p XPS results of 18CuO/CZ before (a) and after (b) reduction at 195 °C.

consistent with XRD quantitative result and the value expected by incorporation model.

To investigate the reduction product of the samples, XPS is used to characterize the 18CuO/CZ catalyst before and after reduction at 195 °C, i.e. the end reduction temperature of the first peak in the TPR profile, as shown in Fig. 7. As known to all, the presence and absence of satellite peaks are the discrimination for Cu^{2+} and the low valence of copper species, respectively [33,34]. The ratio of intensities of the satellite peaks to those of the principal peaks (I_{sat}/I_{pp}) can be used to estimate whether the Cu^{2+} species was reduced. The I_{sat}/I_{pp} values of 18CuO/CZ before and after reduction are about 0.56 and 0.50, respectively, and the binding energy of $Cu2p_{3/2}$ shifts from 933.0 to 932.5 eV, accordingly, some of Cu^{2+} species is reduced. Combined with the results from TPR that the ratio of the area of the first peak and the second peak is almost constant, it could be concluded that the dispersed Cu^{2+} species in CuO/CZ would be stepwise reduced.

The catalytic activities of CO oxidation over a series of CuO/CZ samples are tested at 100 and 125 °C and shown in Fig. 8. When increasing the loading amount of CuO, the CO percentage conversion increases at first and decreases subsequently, indicating that increasing the CuO loading cannot always promote the catalytic activity and a maximum reaches at the suitable copper loading. Among the CuO/CZ samples, the CO percentage conversion of 12CuO/CZ is the highest. According to the results of XRD and TPR, there are both dispersed and small particle of copper oxide species in 12CuO/CZ sample. The results suggest that the active species in this system should be mainly the surface and/or small particle of copper oxide species, which is consistent with the results proposed by Liu et al. that copper entities active for the CO oxidation involved the small CuO particle [35], however, the formation of larger CuO particle does not have contribution to the catalytic activity. In addition, for all catalysts, when the reaction temperature is 125 °C, the CO conversion is about three times as high as that at 100 °C. This result indicates that the catalytic activity of the CuO/CZ for the CO oxidation is influenced greatly by the reaction temperature.

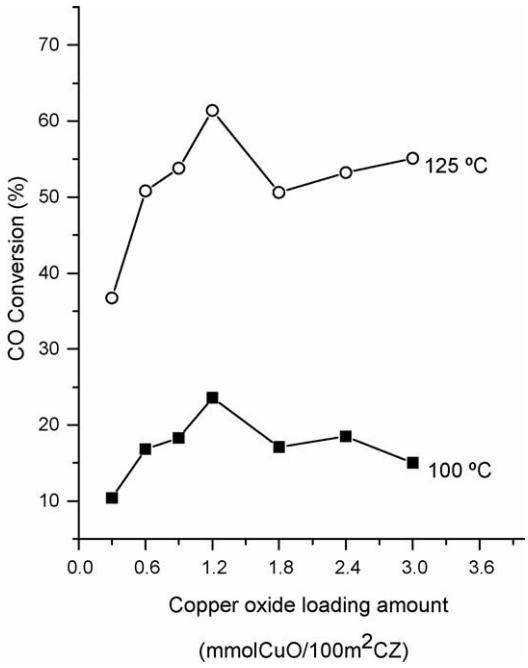

Fig. 8. The catalytic activities of CuO/CZ catalysts.

As reported elsewhere, for copper and ceria-containing catalysts, the higher redox activity of copper-support interface sites on the catalyst played an important role in the low temperature CO oxidation [24]. When the CuO loading amount exceeded a definite value, the particles of bulk CuO formed, which could in part cover the active catalyst surface. This would reduce the catalytic activity, since bulk CuO is known to be an insulator and contribute very little to the total active area and the synergetic effect between the ceria and the copper oxide phase would be prevented [12,36]. In addition, it has also been suggested that the monoclinic distortion of the fully oxidized tenorite CuO phase destroys an epitaxial relationship to the ceria support, preventing an effective transfer of oxygen, and hence, showing lower catalytic activity [37]. Along this line, it may be concluded that when the size of CuO particles in an appropriate region, existing the Cu–Ce–Zr synergism in the reaction, but if the Cu loading exceeds, the CuO cover the surface of the support or formed the large CuO particles, which result in the activity decreasing. Furthermore, it seems to propose that, at current experiment conditions, the optimal copper oxide loading should be controlled around 1.2 mmolCuO/100 m^2CZ.

4. Conclusion

(1) From the XRD and TPR results, the dispersion capacity of copper oxide in CuO/CZ is about 0.70 mmolCuO/100 m^2CZ.
(2) In the CO oxidation reaction, the CuO/CZ catalysts show high activity at low temperature (125 °C) and the active species in this system should be mainly the surface and/or small particle of copper oxide species. Accordingly, the optimal copper oxide loading should be controlled around 1.2 mmolCuO/100 m^2CZ at current conditions.

Acknowledgments

The financial supports of the National Natural Science Foundation of China (No. 20573053), the Specialized Research Fund for the Doctoral Program of Higher Education (No. 20030284002), and the National Basic Research Program of China (Grant No. 2003CB615804) are gratefully acknowledged.

References

[1] K. Min, M.W. Song, C.H. Lee, Appl. Catal. A 251 (2003) 143.
[2] J. Guzman, S. Carrettin, A. Corma, J. Am. Chem. Soc. 127 (2005) 3286.
[3] K. Arnby, A. Torncrona, B. Andersson, M. Skoglundh, J. Catal. 221 (2004) 252.
[4] H.Q. Zhu, Z.F. Qin, W.J. Shan, W.J. Shen, J.G. Wang, J. Catal. 233 (2005) 41.
[5] M. Okumura, N. Masuyama, E. Konishi, S. Ichikawa, T. Akita, J. Catal. 208 (2002) 485.
[6] M.M. Mohamed, S.M.A. Katib, Appl. Catal. A 287 (2005) 236.
[7] F. Grillo, M.M. Natile, A. Glisenti, Appl. Catal. B 48 (2004) 267.
[8] A. Szegedi, M. Hegedus, J.L. Margitfalvi, I. Kiricsi, Chem. Commun. (2005) 1441.
[9] X.C. Zheng, S.H. Wu, S.P. Wang, S.R. Wang, S.M. Zhang, W.P. Huang, Appl. Catal. A 283 (2005) 217.
[10] B. Solsona, G.J. Hutchings, T. Garcia, S.H. Taylor, New J. Chem. 28 (2004) 708.
[11] A. Martínez-Arias, M. Fernández-García, O. Galvez, J.M. Coronado, J.A. Anderson, J.C. Conesa, J. Soria, G. Munuera, J. Catal. 195 (2000) 207.
[12] W. Liu, M. Flytzani-Stephanopoulos, J. Catal. 153 (1995) 304.
[13] R. Burch, J.P. Breen, F.C. Meunier, Appl. Catal. B 39 (2002) 283.
[14] A. Trovarelli, Catal. Rev. 38 (1996) 439.
[15] J. KaŠpar, P. Fornasiero, M. Graziani, Catal. Today 50 (1999) 285.
[16] D. Terribile, A. Trovarelli, J. Llorca, C.D. Leitenburg, G. Dolcetti, Catal. Today 43 (1998) 79.
[17] S.P. Wang, X.C. Zheng, X.Y. Wang, S.R. Wang, S.M. Zhang, L.H. Yu, W.P. Huang, S.H. Wua, Catal. Lett. 105 (2005) 163.
[18] A. Trovarelli, F. Zamar, J. Llorca, C.D. Leitenburg, G. Dolcetti, J. Kiss, J. Catal. 169 (1997) 490.
[19] P. Fornasiero, G. Balducci, R.D. Monte, J. KaŠpar, V. Sergo, G. Gubitosa, A. Ferrero, M. Graziani, J. Catal. 164 (1996) 173.
[20] H. Wang, J.M. Zhu, J.J. Zhu, L.M. Yuan, H.Y. Chen., Langmuir 19 (2003) 10993.
[21] Y.K. Hwang, J.S. Chang, S.E. Park, D.S. Kim, Y.U. Kwon, S.H. Jhung, J.S. Hwang, M.S. Park, Angew. Chem. Int. Ed. 44 (2005) 556.
[22] Y.J. Zhu, W.W. Wang, R.J. Qi, X.L. Hu, Angew. Chem. Int. Ed. 43 (2004) 1410.
[23] H.S. Potdar, S.B. Deshpande, A.S. Deshpande, S.P. Gokhale, S.K. Date, Y.B. Khollam, A.J. Patil, Mater. Chem. Phys. 74 (2002) 306.
[24] A. Martínez-Arias, M. Fernández-García, A.B. Hungria, A. Iglesias-Juez, O. Galvez, J.A. Anderson, J.C. Conesa, J. Soria, G. Munuera, J. Catal. 214 (2003) 261.
[25] A. Martínez-Arias, M. Fernández-García, V. Ballesteros, L.N. Salamanca, J.C. Conesa, J.C. Conesa, C. Otero, J. Soria, Langmuir 15 (1999) 4796.
[26] X.W. Li, M.M. Shen, X. Hong, H.Y. Zhu, F. Gao, Y. Kong, L. Dong, Y. Chen, J. Phys. Chem. B 109 (2005) 3949.
[27] Y. Chen, L.F. Zhang, Catal. Lett. 12 (1992) 51.
[28] L. Dong, Y. Chen, Chin. J. Inorg. Chem. 16 (2000) 250.
[29] Z. Liu, Y. Chen, J. Catal. 177 (1998) 314.
[30] H.Y. Zhu, Y. Wu, X. Zhao, H.Q. Wan, L.J. Yang, J.M. Hong, Q. Yu, L. Dong, Y. Chen, C. Jian, J. Wei, P.H. Xu, J. Mol. Catal. A 243 (2006) 24.
[31] (a) P. Zimmer, A. Tschöpe, R. Birringer, J. Catal. 205 (2002) 339; (b) L. Dong, Y.S. Jin, Y. Chen, Sci. China Ser. B 40 (1997) 24.
[32] N.W. Hurst, S. Gentry, A. Jones, Catal. Rev. 24 (1982) 233.
[33] D.C. Frost, A. Ishitani, C.A. McDowell, Mol. Phys. 24 (1972) 861.
[34] S. Evans, J. Chem. Soc. Faraday Trans. II 71 (1975) 1044.
[35] W. Liu, A.F. Sarofim, M. Flytzani-Stephanopoulos, Chem. Eng. Sci. 49 (1994) 4871.
[36] W. Liu, M. Flytzani-Stephanopoulos, J. Catal. 153 (1995) 317.
[37] B. Skårman, L.R. Wallenberg, P.O. Larsson, A. Andersson, J.O. Bovin, S.N. Jacobsen, U. Helmersson, J. Catal. 181 (1999) 6.